Measurement of the Non-Common Vertex Error of a Double Corner Cube

Alireza Azizi[*a], Martin Marcin[a], Douglas Moore[a], Steve Moser[a], John Negron[a], Eung-Gi Paek[b], Daniel Ryan, Alex Abramovici[a], Paul Best[a], Ian Crossfield[a], Bijan Nemati[a], Tim Neville[a], B. Platt[a], Leonard Wayne[a]
[a]Jet Propulsion Laboratory, 4800 Oak Grove Dr, Pasadena, CA 91109
[b]Naval Research Laboratory 4555 Overlook Ave. S.W. Washington, DC 20375

ABSTRACT

The Space Interferometry Mission (SIM) requires the control of the optical path of each interferometer with picometer accuracy. Laser metrology gauges are used to measure the path lengths to the fiiducial corner cubes at the siderostats. Due to the geometry of SIM a single corner cube does not have sufficient acceptance angle to work with all the gauges. Therefore SIM employs a double corner cube. Current fabrication methods are in fact not capable of producing such a double corner cube with vertices having sufficient commonality. The plan for SIM is to measure the non-commonalty of the vertices and correct for the error in orbit. SIM requires that the non-common vertex error (NCVE) of the double corner cube to be less than 6 µm. The required accuracy for the knowledge of the NCVE is less than 1 µm. This paper explains a method of measuring non-common vertices of a brassboard double corner cube with sub-micron accuracy. The results of such a measurement will be presented.

Keywords: non-common vertex, double corner cube, interferometry, SIM, metrology

1. INTRODUCTION

The Space Interferometry Mission (SIM), currently under development at the Jet Propulsion Laboratory, consists of three 9-meter baseline interferometers mounted onto a flexible truss[1]. SIM's science goals require 1µas accuracy in its astrometric measurements. To achieve this level of accuracy, it is necessary to have picometer class sensitivity in controlling the optical path of each interferometer. SIM uses an external metrology systems consisting of 14 beam launchers to measure absolute length and relative variations in the baseline of the interferometer[2]. Ideally a design with a single corner cube would be preferred because then all gauges that interrogate the fiducial would see the same characteristics. However the geometry of SIM requires a fiducial with greater angular acceptance to accommodate the widely spaced gauges. As a result, SIM will employ multiple corner cubes with either two or three retro-reflectors sharing a "common" vertex.

Current fabrication methods are not capable of producing a double corner cube with vertices coincident to such a level that SIM's external metrology system will be insensitive to alignment error. This error causes both a field dependent error and a bias error in the absolute metrology.

The double corner cube which can currently be produced will give rise to measurement errors due to non-commonality of the individual vertices. When the SIM makes narrow angle field measurement, the instrument sequentially views a group of reference stars spread over a half degree on the sky and target star within field. The double corner cube which is mounted to the siderostat slews while making these measurements. The non-common vertex will cause an error in the interferometer baseline measurement. This error will propagate to a field dependent error in the star position. The absolute metrology system of SIM is used to measure the length of the legs in the truss to within 3µm. Since the two

[*] alireza.azizi@jpl.nasa.ov ; phone:818-354-0639; fax: 818-393-4357

beam's paths into the double corner cube are directed at different vertices, the non-commonality of vertices will directly affect the absolute metrology measurement.

SIM requires that the non-common vertex error (NCVE) for the double corner cube to be less than 6 µm. The accuracy for the knowledge of the NCVE is required to be less than 1 µm. The present plan is to measure the non-commonalty of the vertices and correct for the error in orbit. Figure 1 shows a double corner cube at the location of one of the siderostats and an exaggerated view of the misaligned vertices.

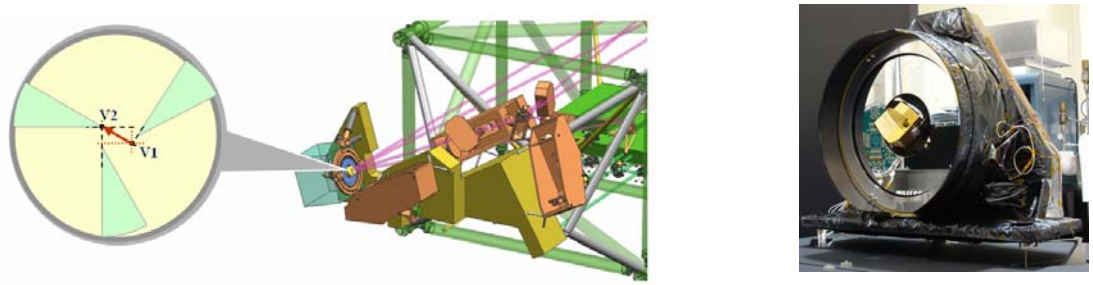

(a) (b)

Fig. 1. (a) Expanded picture of the double corner cube in the siderostat, (b) a double corner cube inside a test siderostate.

2. NCVE CONCEPT

A Double Corner Cube (DCC) consists of two hollow corner cubes (CC1 and CC2) which provide a wider viewing angle. The two corner cubes are made by mounting three 30° wedge prisms on a common base plate as shown in Figure 2.

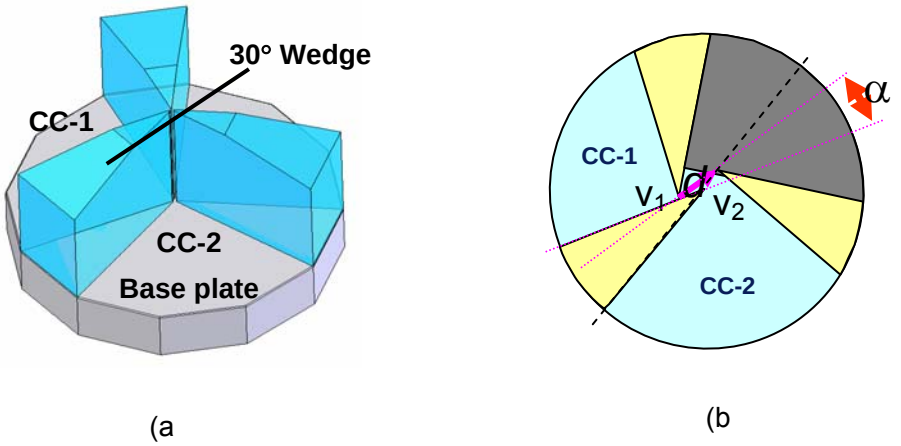

Fig. 2. a) isometric view of a double corner cube b) Top view of the Non-Common Error (NCVE) of a DCC.

The separation of these two vertices can be characterized by its magnitude (d) and its direction (α) in polar coordinates. Alternatively, NCVE may also be expressed in terms of its Cartesian coordinates.

The NCVE measurement concept is to fix one vertex and monitor the motion of the second vertex as the DCC is rotated about the axis normal to the base plate. In this method the DCC under test rotates about one of the vertices (e.g. V_2) with the rotation axis normal to the base plate. At each rotation angle the change in distance between vertex V_1 and a fixed corner cube (CC) is measured. The beam launcher, the fixed corner cube and its electronics comprise a metrology gauge. Since there is a fixed corner cube, the observed motion detected by the beam launcher is due solely to the motion of

vertex V_1. For redundancy there are two gauges actively monitoring the motion of the vertex. Figure 3 shows the schematic concept of the measurement method. The relation between the optical path difference (OPD) due to the rotation φ and NCVE (d) can be written as follows:

$$|d| = \frac{OPD}{4\sin(\frac{\phi}{2})\sin(\Theta)\left(\sin(\frac{\varphi}{2}+\beta)\cos\Phi - \cos(\frac{\varphi}{2}+\beta)\sin\Phi\right)} \quad (1)$$

Where Θ and Φ are the polar and azimuthal angles of the interrogating gauge and β is the clocking angle of the NCVE vector in the frame of the gauge.

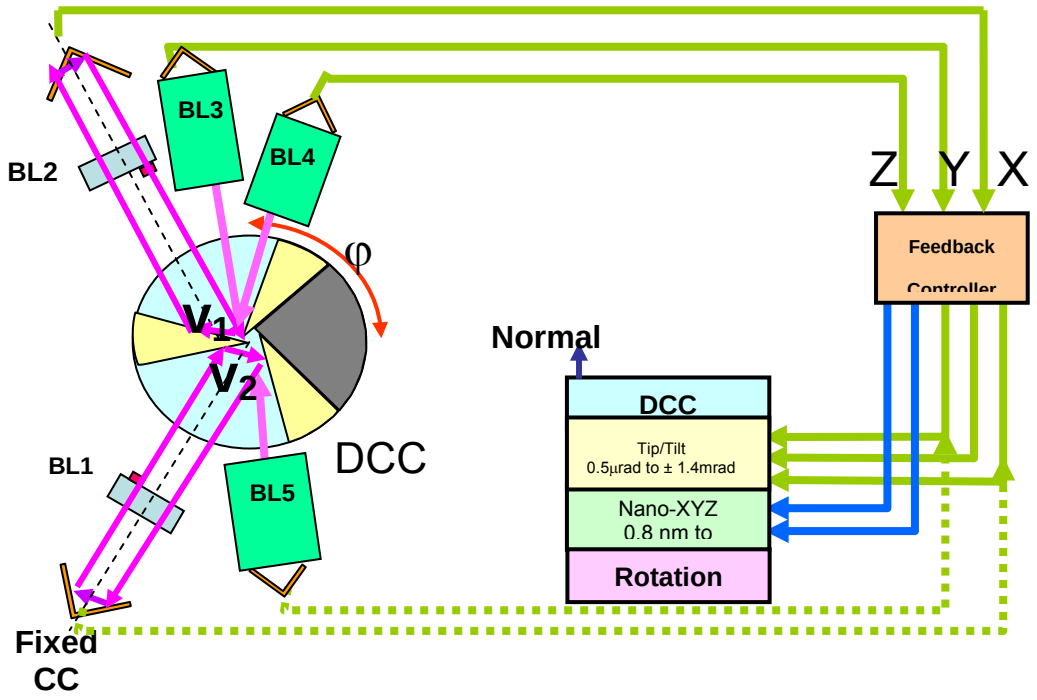

Fig. 3. NCVE measurement method block diagram.

The motion of the rotation stage is not perfect. It is accompanied by wobbling and runout effects which results in motion of the entire DCC. To compensate for imperfections in the rotation stage, three metrology gauges measure the motion of vertex V_2. A feedback control system uses the three gauge measurements to determine the correction to be applied to bring V_2 back to its original position.

3. SYSTEM DESCRIPTION

The NCVE testbed consists of the following subsystems: mechanical, metrology laser source, beam launchers, electronics, software control and data collection. Details of all the subsystems have been given in other publication[3]. Some of the critical subsystems will be mentioned below. To increase the sensitivity of the testbed to permit sub-micron measurements the testbed resides in a vacuum chamber to reduce atmospheric influences. The chamber is not floating but it does rest on an isolation pads within the lab. In addition the breadboard inside the chamber is setup on three isolation pads.

3.1 Mechanical Setup

The NCVE testbed structural components are built of Super Invar components because of its low coefficient of thermal expansion to eliminate or reduce any optical path changes due to thermal effect. Beyond this, adverse thermal effects were also addressed by designing an athermalizing system. Athermalization cancels residual thermal expansion of contraction.

The orientation of each beam launcher was carefully selected to insure that they are not coplanar and providing the maximum angular coverage when the DCC rotates. The knowledge of the location of each beam launcher is important for the extraction of the NCVE measurement. Therefore a special alignment procedure was followed during beam launcher alignment. The next section will explain the alignment method for the beam launcher. Figure 4 shows the mechanical setup with the DCC mounted on the translation stage stack in the center and the truss supporting the beam launchers.

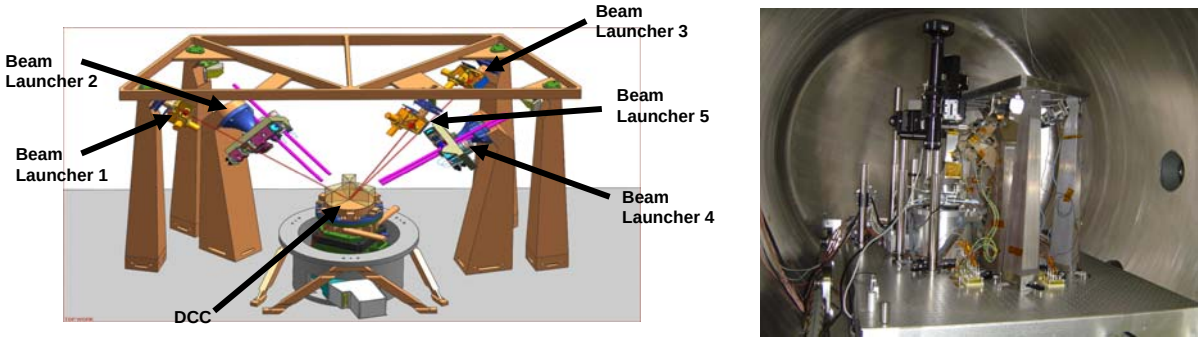

Fig. 4. NCVE testbed beam launcher truss and DCC

To compensate for imperfections in the rotation stage and fix the position of vertex V_2 to its original position, active alignment in tip/tilt and the xyz directions is needed. This is achieved with a non-xyz stage, and a tip/tilt stage stacked on top of the rotation stage. Figure 5 shows the DCC on top of the translation stage stack. Table 1 gives the range and resolution of each stage.

Table 1. Specification of all the stages

Stage Type	**Manufacturer**	**Model #(part#)**	**Resolution**	**Range**	**Driven**
Rotation	Newport	RV120 PEV6	.001 deg	+/- 175 deg	Stepper
Coarse X	JPL	METFIDMNT07_A2	<50 um	+/- 0.5mm	Manual
Coarse Y	JPL	METFIDMNT06_A2	<50 um	+/-0.5 mm	Manual
nano-stage XYZ	PI	P561.3VD	0.2 nm	100,100,100 um	Piezo
Tip/Tilt	PI	M044.D01	< 1 mrad 0.23 urad	+/- 7 deg +/-1.4 mrad	Manual PZT

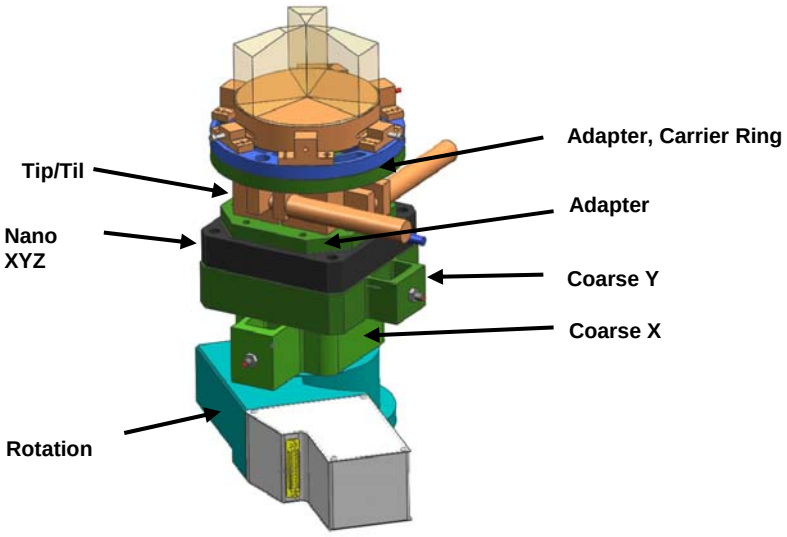

Fig. 5. DCC and the mechanical stack

3.2 Laser source

A 100mW laser at 1319 nm wavelength is used as the metrology source. To provide a heterodyne signal, the laser beam is split into two beams which are then frequency shifted with a difference of 20 KHz using two acousto-optic modulators. Interfering these beams within the beam launchers produces the 20 KHz heterodyne signal. Two fibers carry the frequency-shifted signals to the chamber. A pair of 1X8 beam splitters distributes the signals to each of the five beam launchers.

3.3 Beam launchers

Two different type of beam launchers are used in this testbed. In the first type, the two beams (reference and measurement) are spatially separated and follow a racetrack path between the corner cubes. In the second type, separation of the two beams is accomplished via their polarizations (S and P). The beams from these beam launchers travel from corner cube vertex to corner cube vertex. The conceptual design of these two types of beam launchers is shown in figures 6 and 7.

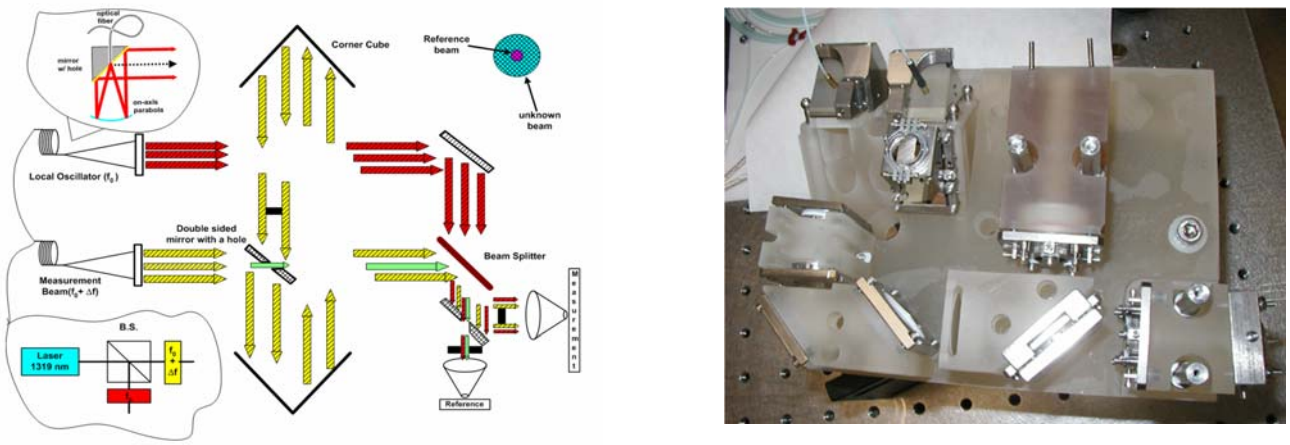

Fig 6. Racetrack beam launcher

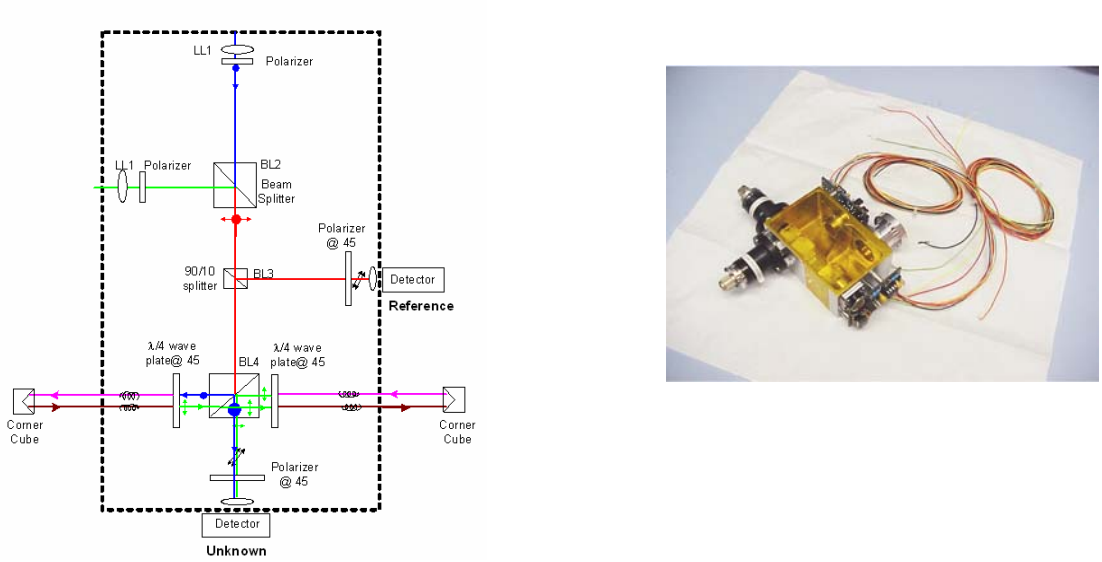

Fig 7. Vertex-to-vertex beam launcher

4. ALIGNMENT

As mentioned previously, the alignment of the beam launchers and DCC is critical to the measurement of the NCVE. A brief explanation of the alignment procedure follows.

4.1 Tip/tilt adjustment

The tip/tilt of the DCC base plate is minimized so the rotation of the DCC is about the vertical axis. An autocollimator is used to measure the amount of tip/tilt of the DCC base plate. An autocollimator was setup to view vertically downward at the DCC base plate. As the DCC rotates, the autocollimator monitors the tip/tilt of the base plate. Based on the autocollimator readings the tip/tilt of DCC is reduced to the desired level. In practice it was straight forward to achieve less than 5 arcseconds while the error budget required less than 50 arcseconds.

4.2 Alignment of the DCC vertex with the center of rotation

Key to the NCVE measurement techniques is the need to place one of the vertices at or close to the center of rotation. A microscope with CDD camera was used to monitor one of the vertices while the DCC was rotated beneath it. Using the coarse x-y stage, and the nano-xyz stage one vertex was moved as close as possible to the center of rotation.

4.3 Beam launchers polar and azimuthal angles alignment

Accurate measurement of the NCVE requires precise knowledge of the beam launcher orientation specifically their polar and azimuthal angles. It is easier and more precise to set the beam launchers at known coordinates. The vertex-to-vertex nature of beam launchers 1 and 3 allows the setting of the polar and azimuthal angles very precisely. The coordinates of the rest of the beam launchers can be measured using the motion of the nano-xyz stage. The procedure for setting and measuring the polar and azimuthal angles will be explained below.

4.3.1 Setting the polar angle for beam launcher 1 and 3

A cube with a 30° prism attached to it was used to set the polar angles of beam launcher 1 and 3. Figure 8 shows a picture of the cube/prism assembly and schematic of the setup. The bottom of the cube is 50% reflective and the surface of the 30° prism is fully reflective. This assembly allows one to set the polar angles of beam launcher 1 and 3 to 60 ± 0.03 degrees.

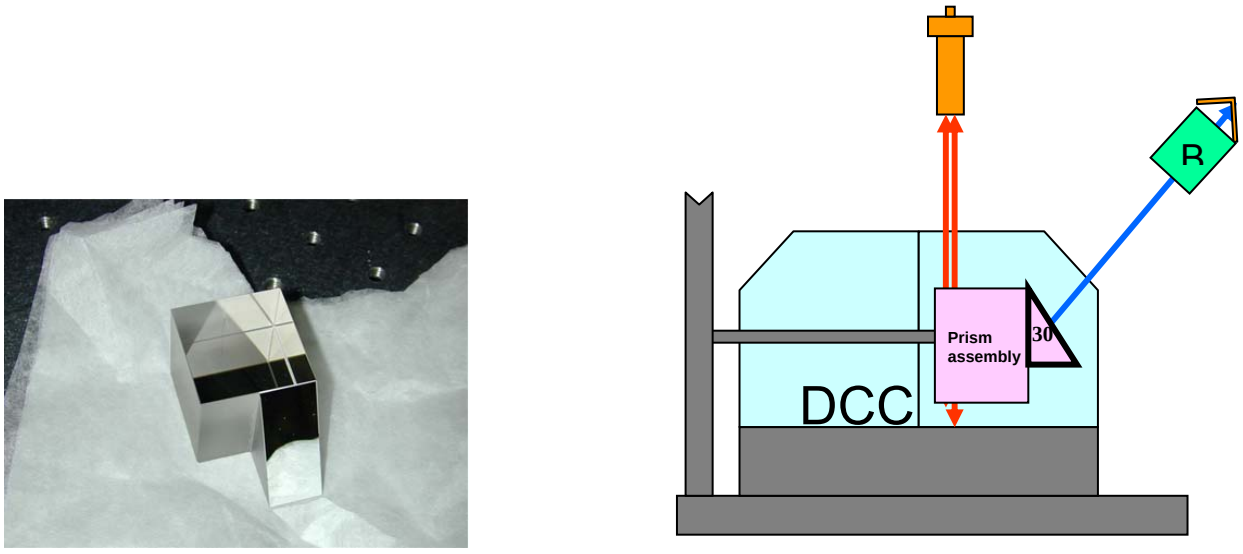

(a) (b)

Fig. 8. (a) Cube/prism assembly, (b) schematic setup of the prism assembly with DCC

First the cube/prism assembly is positioned above the DCC such that the beam from the beam launcher strikes the reflective surface of the 30° prism. Then using an autocollimator the cube/prism assembly is adjusted until it is parallel with the baseplate of the DCC. Finally the tip/tilt of the beam launcher is adjusted to get a strong heterodyne signal. This procedure sets the polar angle of the beam launcher to 60 degrees.

4.3.2 Setting the azimuthal angle

Azimuthal angles of the beam launchers are defined in the laboratory coordinate system. The laboratory coordinate system is defined as initial specific orientation of the DCC. The Z direction is normal to the DCC base plate. The X direction is the projection of the beam from launcher 1 onto the plane of the base plate when the middle wedge and the base plate appear as a roof mirror to launcher 1. The X axis intersects the center of rotation. The X axis is defined using beam launcher 1 and a rhomboid prism. This method allows the azimuthal angle for beam launcher 1 to be set to 180 degrees ± 0.02 milliradians.

After positioning the rhomboid prism in front of beam launcher 1, the DCC is rotated until a strong heterodyne signal is optained. The face of the middle wedge is now perpendicular to the projection of launcher 1's beam on the plane of the base plate. With beam launcher 1 and the DCC in this orientation the azimuthal angle is defined to be zero (180º in the lab frame). Figure 9 shows pictorial description of the above process.

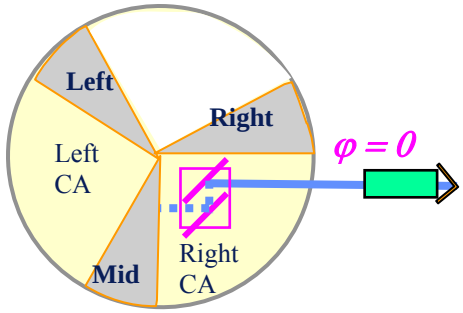

Fig. 9. Setting the azimuthal angle

4.3.3 Measurement of the remaining beam launcher polar and azimuthal angles

In principle, one could move the DCC a known amount using the nano-xyz stage and monitor the gauge readings to determine the beam launcher orientations. This procedure is complicated by the fact that the nano-xyz stage axes are rotated relative to the lab frame being established. Fortunately the polar and azimuthal angles for beam launcher 1 *are* known. This allows the clocking of the nano-xyz stage relative to the lab frame to be determined. With the clocking angle known, one can extend the procedure to the remaining beam launchers.

5. NCVE MEASUREMENT

With the location of the beam launchers known, the testbed is ready for the NCVE measurement. The data logging and control are automated. The DCC rotated 20 degrees to start the measurement sequence. This offset maximized the angular coverage. Subsequent measurement were taken at 2º increments. At each measurement angle the control algorithm uses the data from beam launchers 3,4 and 5 to correct for the unwanted motion of the vertex 2. The nano-xyz stage is commanded to move vertex 2 back to the center of rotation. Once there, beam launchers 1 and 2 collect the phase date for NCVE analysis.

In order to minimize the effect of low frequency noise and thermal drift, a "chopping" method is employed. The benefit of chopping is that the noise on the data is severely reduced because the DCC is returned to its initial position on every other measurement. Therefore the home position is repeatedly monitored allowing the noise to be modeled and removed. Figure 10 shows the progression of the measurements using the chopping algorithm. 40 seconds of delay prior to measurement allowed the stages to settle. Figure 11 shows a sample of data collected during a run.

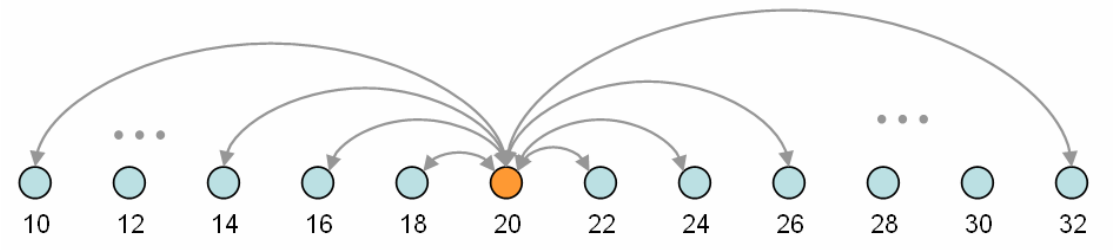

Fig. 10. NCVE fountain chopping scheme. Angles have been changed to absolute values

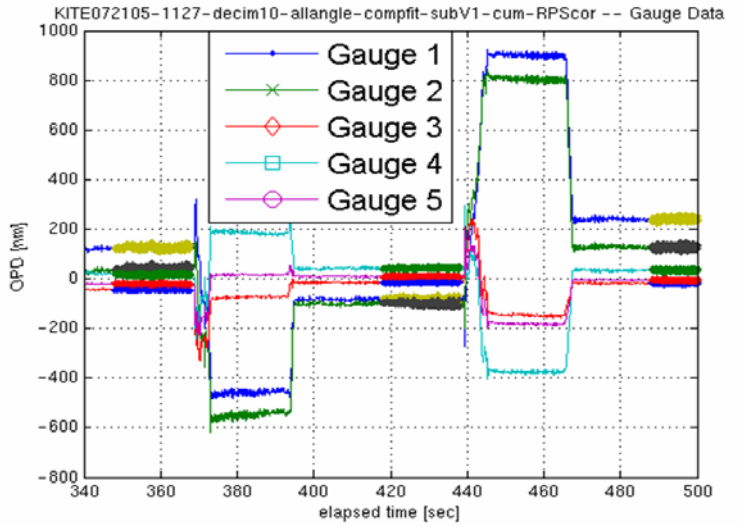

Fig 11. Sample data run with chopping algorithm

6. DATA ANALYSIS

Before calculating the NCVE value several corrections must be made to the data. Monte Carlo and modeling analysis indicated that reflection phase shift (RPS) could be as large as 100 nm for some of the beam launchers (in particular gauge 5). To correct for RPS a model of an individual beam launcher was used to calculate the effect. The value from the model is used to correct each beam launcher at every data point.

The next correction applied uses the chopping algorithm to reduce the effects of long-term drift in the metrology system. The data from each gauge takes the form of a set of N measurements $\{m_1, m_2, m_3, m_4, m_5, \ldots, m_N\}$ at the rotation angles $\{a_0, a_1, a_0, a_2, a_0, \ldots, a_0\}$. These are transformed to a set of (N+1)/2 "measured changes" {0, }, where i = {1, 3, …, N-2}, at the rotation angles {a0, a1, a2, a3, …, a(N-1)/2}.

The final correction made accounts for the undesired motions of the DCC Vertex 2 (V_2) in the lab frame of reference. In an ideal NCVE measurement system, V_2 would remain motionless in the lab frame as the DCC rotated about it. However, even with the correction during the test some residual motion remains. Gauges 3, 4, and 5 are used to estimate V_2's position and remove its residual translation from all the gauge data. V_2's motion has three degrees of freedom, and the distance from it to the stationary corner cubes is measured by gauges 3, 4, and 5. Thus V_2's position is fully determined by these three gauges measurements. V_2's position at every angle step is calculated, and the projection of that motion along each gauge direction is used to correct each data point. Thus, we calculate:

$$\vec{V}_2 = \vec{V}_2(g_{3,} g_4, g_5) \tag{2}$$

Then the corrected gauge reading is:

$$g_i^C = g_i - \hat{u}_i . \vec{V}_2 \tag{3}$$

In the equation above i = {1, 2, 3, 4, 5} and $\hat{u}_i$ is a unit vector in the direction of gauge i. Additionally, because the position of vertex 2 (V_2) is determined precisely by Gauges 3, 4, and 5, this correction has the effect of setting all the data from those three gauges to zero. Figure 12 shows a data set before and after correction.

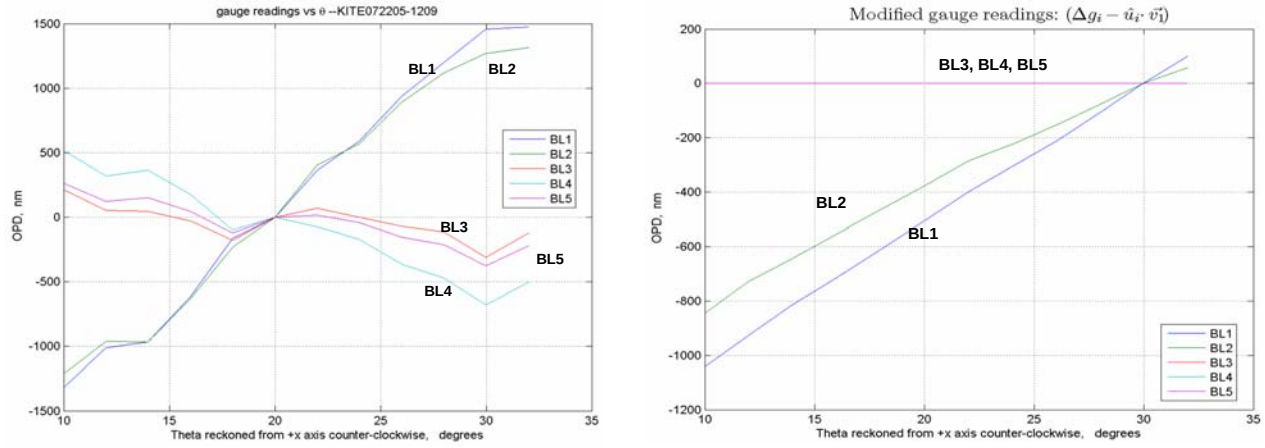

(a) (b)

Fig 12. (a) A set of data with averaged, and chopped gauge data corrected at each rotation step (b) Data with residual motion of V_2 subtracted.

6.1 Fitting the data

The corrected data can be fit for gauge 1, 2 or both combined using a model of uniform circular motion to determine the two NCVE vector components. We can use this method to fit data from all five gauges at once, producing our most precise estimate of the NCVE.
Assuming a pure rotation around V_2 and using the notation above, the components of the NCVE in the lab frame at each angle step θ_i are given by

$$\vec{d}^{\,T}(\theta_i) = \begin{bmatrix} d^T \cos(\theta_i + \varphi^T) \\ d^T \sin(\theta_i + \varphi^T) \\ 0 \end{bmatrix} \tag{4}$$

The superscript ^{T} indicates that this is the theoretically 'true' measurement. Given a particular NCVE magnitude and azimuth, the NCVE lab frame components can be computed at each angle step (again, we assume perfect knowledge of our rotation angle). A relative metrology gauge sees only the projection of this motion along its direction.

$$g_j^T(\theta_i, d^T, \varphi^T) = \hat{u}_j \cdot \vec{d}^{\,T}(\theta_i) \tag{5}$$

Because the metrology gauges measure only relative displacement, there is an additional offset constant C that must also be fit. Thus the final fit is a minimization of the sum to find the three parameters d^T, φ^T, and C using the rotation angles θ_i and the corrected data from the j^{th} gauge, i.e.

$$\sum_i \left(g_j^c(\theta_i) - g_j^T(\theta_i, d^T, \varphi^T) - C \right)^2 \tag{6}$$

Figure 13 shows results of fit for many runs using the fit method.

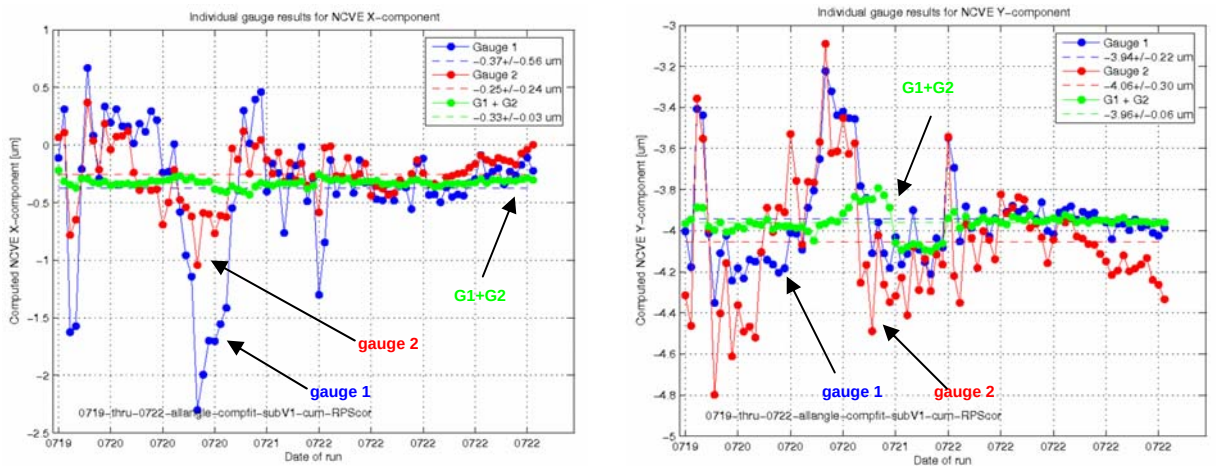

Fig. 13 Shows NCVE X and Y components with all the corrections using only gauge 1(blue), using only gauge 2 (red) and using both gauges in a combined fit (green).

As the data shows initially there was some fluctuation among the individual gauges over the many runs. With the combined fit the two gauges the fluctuation is reduced. The source of the fluctuation is not clear but could be due to the pump down conditions of the chamber or differences in the control scripts.

7. FINAL RESULTS

The double corner cube used in these measurements was produced by Australia's Commonwealth Scientific and Industrial Research Organization (CSIRO). The final results of the DCC are shown in figure 14. The results with the combination of gauges 1 and 2 shows $NCVE_X$ = -0.32 ± 0.012 µm and $NCVE_Y$ = -3.96 ± 0.006 µm. The circles shows results from several different runs.

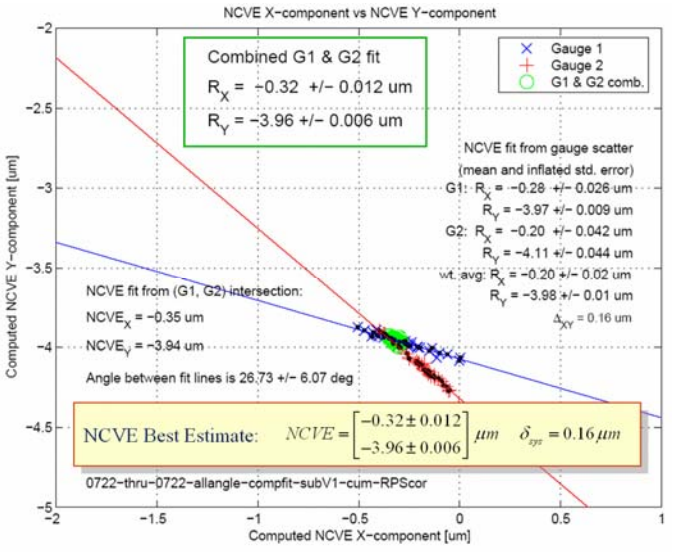

Fig 14. The NCVE results

8. ACKNOWLEDGEMENTS

The research described in this paper was carried out at the Jet Propulsion Laboratory, California Institute of Technology, under a contract with the National Aeronautics and Space Administration.

9. REFERENCES

1. J. Marr, "Space Interferometry Mission (SIM) overview and current status," *SPIE conference on Interferometry in Space*, vol. 4852, Hawaii, August 2002.

2. A. Azizi, O. Alvarez-Salazar, R. Goullioud, Y. Gursel, " Metrology System for Space Interferometry Mission Testbed 3", CLEO/QEC & PhAST Technical Digest on CD ROM (The Optical Society of America, Washington DC), CTu06, San Francisco, 2004

3. JPL internal document "The Non-Common Vertex Error testbed Results Document", SIM-Lib File-132580, 10/27/05.